

---

# Winning the lottery with neurobiology: faster learning on many cognitive tasks with fixed sparse RNNs

---

**Mikail Khona\***  
Physics  
MIT  
mikail@mit.edu

**Sarthak Chandra\***  
Brain and Cognitive Sciences  
MIT  
sarthakc@mit.edu

**Joy J. Ma**  
Physics  
MIT  
joym@mit.edu

**Ila Rani Fiete**  
Brain and Cognitive Sciences  
MIT  
fiete@mit.edu

## Abstract

RNNs are often used as models of biological brain circuits and can solve a variety of difficult problems requiring memory, error-correction, or selection [10, 26, 25]. However, fully-connected RNNs contrast structurally with their biological counterparts, which are extremely sparse ( $\sim 0.1\%$ ). Practical deployment of large RNNs is often limited due to requirements of long training times and large memory requirements. Motivated by brains, where neural connectivity is constrained by distance along cortical sheets and other synaptic wiring costs, we introduce locality masked RNNs (LM-RNNs) that utilize task-agnostic predetermined graphs with sparsity as low as 4%. We make three contributions: First, we show that LM-RNNs can perform as well as their fully-connected counterparts, without *a posteriori* construction of the best sparse subnetwork. Second, we find that LM-RNNs train faster with more data-efficiency in a multitask setting relevant to cognitive systems neuroscience, often achieving better asymptotic performance. Third, we contribute a new cognitive multi-task battery, Mod-Cog, consisting of 132 tasks that expands by  $\sim 7$ -fold the number of tasks and task-complexity of an existing commonly used set of tasks [39], showing that while LM-RNNs can solve the simple [39] tasks with a small pool of unconnected autapses, the expanded task-set produces richer solutions.

## 1 Introduction

As models get more complex and larger, various techniques have been developed to tackle the problem of prohibitively large resources required to train and deploy these models. Several methods have tried to get around this issue using techniques like pruning, first introduced in [18, 31, 13], low-rank approximation[11] and distillation[9]. These results demonstrate that it is in principle possible to have equally good solutions with far fewer parameters. However there do not exist any computationally cheap methods to find these solutions.

Inspired by neuroscience, we modify the architecture of a vanilla fully-connected RNN in one particular fashion — noting that neurons in the brain are arranged on two-dimensional cortical sheets and wiring length costs constrain connectivity, we construct a fixed sparse graph chosen by allowing local connections among neurons laid on a two-dimensional sheet. We then use this graph for the

RNN, by only training weights between nodes that correspond to edges on the graph, and setting all other weights to zero. We refer to an RNN in this set up as a ‘Locality Masked RNN’ (LM-RNN). Another motivation for our work comes from modeling grid cell networks in systems neuroscience [15], where it was shown analytically that fixed and local topographic connectivity encouraged the formation of modules.

Exploiting such simple locality constraints in LM-RNNs, when applied to multitask regimes relevant to cognitive systems neuroscience, results in distinct advantages: these networks require far fewer parameters to train, there is no cost to performance relative to an unconstrained network, and in fact learning is more rapid, sample-efficient and can achieve higher asymptotic performance. In contrast to other works in this domain, we do not need any sophisticated pruning methods, any algorithms to construct and modify sparse skeletons nor any training data.

We focus our results on multitasking regimes for RNNs, by training them to simultaneously learn many cognitive tasks. We expect our results on the improvements conferred by LM-RNNs to primarily apply in this multitask learning setting, where the recognition of modular structure across tasks is important for generalization and effective learning.

We make 3 main contributions:

- We show that LM-RNNs can perform as well or better than dense networks, when accounting for the total number of nodes or the total number of synapses. Locality masking is thus an efficient prescription for choosing sparse subnetworks in a task agnostic and data independent fashion while still achieving high performance.
- We show that LM-RNNs reach this high performance faster and with lesser training than dense networks, indicating that sparse networks may be preferable to dense networks in memory and data-limited regimes for learning multiple tasks
- We show that the tasks defined in [39] (a commonly used set of 20 tasks[33, 2, 4, 27, 14] to study representations in networks performing many cognitive tasks) can be solved by a small pool of unconnected autapses, which is essentially a feedforward structure. We then introduce Mod-Cog, a large battery consisting of 132 tasks inspired by cognitive science problems such as interval estimation, mental navigation and sequence generation which provides a useful setting to examine multitask learning and representation across tasks relevant to cognitive systems neuroscience.

## 1.1 Related work

Several works have tried to operationalize the idea of sparsity. These methods can be roughly categorized into 2 main classes:

**Dense-to-sparse** Ref. [8] experimentally showed that training followed by pruning and retraining can give sparse networks with no loss of accuracy and ignited an interest in pruning methods. Following this work, the lottery ticket hypothesis states that dense, randomly-initialized, feed-forward networks contain subnetworks (“winning tickets”) that — when trained in isolation — reach test accuracy comparable to the original network in a similar number of iterations [6]. The best method to identify such winning tickets is Iterative Magnitude-based Pruning (IMP) [6, 7], which is computationally expensive and has to be run thoroughly for every different network. It has also been shown that parameters of the sparse initialization distribution and sign of weights at initialization are important factors [40] which determine winning tickets.

Overall, iterative pruning and retraining methods involve 3 steps: (1) pre-training a dense all-to-all model, (2) pruning synapses based on some criteria, and (3) re-training the pruned model to improve performance. This cycle needs to be done at least once and in many cases, multiple times, to get good performance. So this procedure requires at least the same training cost as training a dense model and often even more than that.

Other methods involving ways to encourage sparsity during the training process include  $L_1$  (Lasso) regularization[38],  $L_0$  regularization[23, 35] and pruning weights below a certain threshold which increases during training[32]. Another recent method, STR, smoothly induces sparsity while learning pruning thresholds thereby obtaining a non-uniform sparsity budget[17]. Unfortunately, all of the aforementioned methods require training the original dense network, in varying amounts, thus

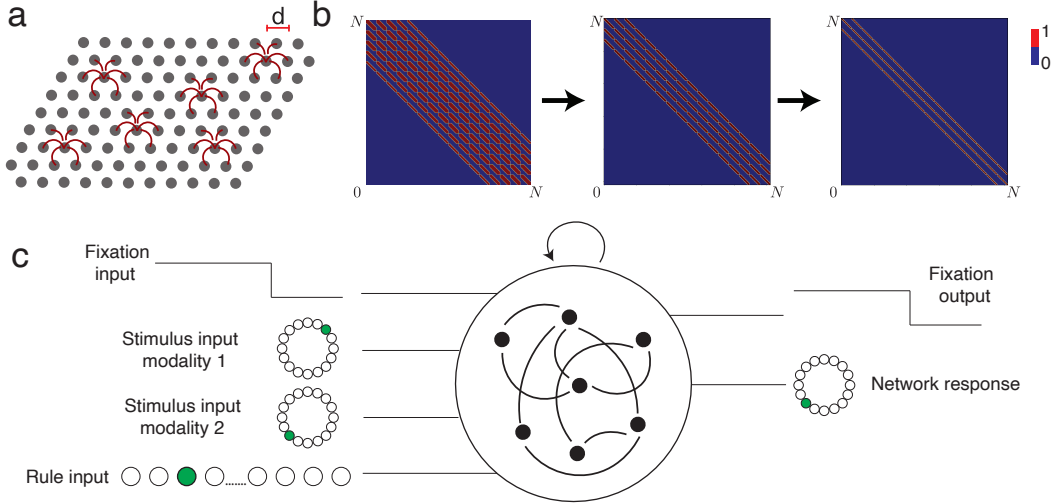


Figure 1: (a) In LM-RNNs neurons are arranged on a two-dimensional sheet, with nonzero weights permitted for nodes up to a distance  $\leq d$  apart. (b) Locality masking on a two-dimensional sheet can be treated as a sparse mask on the hidden-to-hidden weights of an RNN (c) Schematic of the RNN setup in the context of Yang tasks and Mod-Cog: the network receives inputs encoding directions on two rings, a fixation signal and a rule input. The network is trained to output a fixation signal and a direction on a ring of output nodes.

precluding the benefits that can be obtained by having exact sparsity on the computation during training.

A class of methods which do not involve training data like SynFlow[36], GraSP[37], SNIP[19, 20] and FORCE[3] have been studied for only feedforward networks.

In the context of neuroscience, recent work has shown that effective pruning in recurrent networks can be done by biologically plausible algorithms based on noise correlations between the presynaptic and postsynaptic neuron[30].

**Sparse-to-sparse** Another line of work concerning sparse-to-sparse training is most relevant to our study. This involves using a sparse interaction graph which is used to mask gradient updates. Older works maintained a static graph [28] and dealt only with feedforward networks but newer methods such as dynamic sparse training (DST)[5, 22] have been proposed for both feedforward networks and RNNs which dynamically improve the sparse graph and provide better performance. All of these methods involve changing the topology of the sparse graph during training.

Ref. [22] considers Erdos-Renyi (ER) type static sparse RNNs but for relatively denser values of sparsity (0.53 and 0.67) and more complex architectures like stacked LSTMs and RHNs [41]. Here we explore more extreme values of sparsity ( $\sim 5\%$  and below) and show that they are optimal.

Static sparse networks have also found common usage in reservoir computing architectures, where large sparse networks are preferred to fully-connected networks to increase heterogeneity across nodes and allow for “richer” dynamics[12, 24].

## 2 Results

### 2.1 Locality masked RNNs (LM-RNNs)

We restrict ourselves to simple RNNs for interpretability in the context of systems neuroscience. Our RNNs follow dynamics defined by:

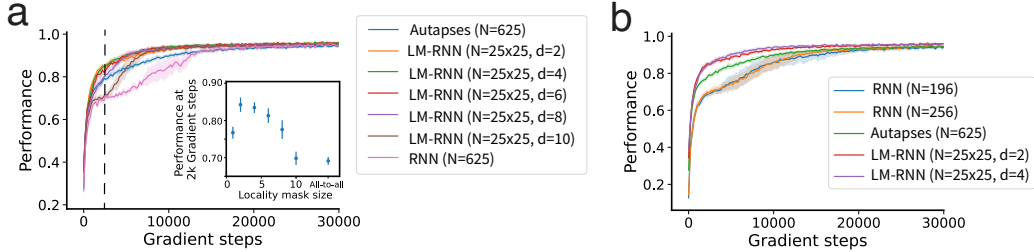


Figure 2: (a) LM-RNNs for all choices of locality mask sizes,  $d$ , perform better than fully-connected RNNs with the same number of nodes. This includes  $d = 0$ , i.e., a disconnected pool of autapses which also outperforms the fully-connected network. *Inset*: performance at  $2 \times 10^3$  gradient steps across different values of  $d$  demonstrates a small optimal  $d$  that leads to the best performance. (b) LM-RNNs also outperform fully-connected RNNs constructed with the same number of synapses. RNN( $N = 196$ ) and RNN( $N = 256$ ) have  $5.2 \times 10^4$  and  $8.3 \times 10^4$  parameters respectively;  $N = 625$  autapses, LM-RNN( $N = 25 \times 25, d = 2$ ) and LM-RNN( $N = 25 \times 25, d = 4$ ) have  $4.4 \times 10^4$ ,  $5.2 \times 10^4$  and  $7.4 \times 10^4$  parameters respectively

$$\begin{aligned}
 h_{t+1} &= (1 - \alpha)h_t + \alpha f(Wh_t + Oi_t + b_i) \\
 o_{t+1} &= Rh_{t+1} + b_o
 \end{aligned}$$

Corresponding to the biological arrangement on neurons on a two-dimensional cortical sheet, we arrange the nodes of an RNN on the lattice points of a two-dimensional plane, as shown in Fig. 1a. Then, we constrain the weights for recurrent connections within the nodes of the RNN to be always zero for pairs nodes that lie at a euclidean distance of larger than  $d$ . The training of the RNN then proceeds in the usual fashion by using back propagation of the loss to update the unconstrained weights. We refer to such an RNN as a Locality masked RNN (LM-RNN). These networks are trained on many cognitive tasks using supervised learning with a cross entropy loss [39] (see Appendix for more details).

In effect, the LM-RNN consists of a sparse subgraph of the fully connected network, with each node connected to the  $\sim \pi d^2$  nearest nodes to it. We posit that this sparse subgraph is a “winning lottery ticket”, such that when trained in isolation the LM-RNN achieves comparable performance to a fully recurrently trained network. Moreover, we will demonstrate that these winning lottery tickets perform better in a more data-efficient manner than fully connected counterparts with a similar number of nodes or a similar number of synapses. This approach can be implemented easily in all training frameworks and is agnostic to the specific optimization algorithm being used.

## 2.2 LM-RNNs learn the ‘Yang tasks’ more rapidly than fully-connected RNNs

We apply LM-RNNs to a dataset used commonly in systems neuroscience, a set of 20 cognitive tasks introduced in [39], which we henceforth refer to as the Yang tasks. Each of these 20 tasks are constructed on the same input stimulus modality — two rings of input units are used that support a single activity bump, encoding a one-dimensional circular variable (which could represent direction of motion, for example). Along with the two rings, two additional inputs are fed into the RNN: first, a one-hot encoded rule input vector, indicating which task is to be performed; and second, a fixation input, a decrease of which is treated a ‘go’ signal for the RNN to provide the appropriate output. The expected output for each task is a response direction, which is again encoded in a ring of output units (which could represent, for example, a reach or saccade direction). A schematic of the setup of the RNN is shown in Fig. 1c. For each trial of each task, the inputs are drawn probabilistically from the same distribution across trials that uniformly samples all input directions across both input modalities.

We compare LM-RNNs with different values of  $d$  against fully-connected RNNs with the same number of neurons (and hence many more parameters; cf. Fig. 2a) and fully-connected RNNs of a smaller size but with the same number of parameters (cf. Fig. 2b). In all cases, LM-RNNs for *any* value of  $d$  are far more sample-efficient and learn the tasks with same asymptotic performance as

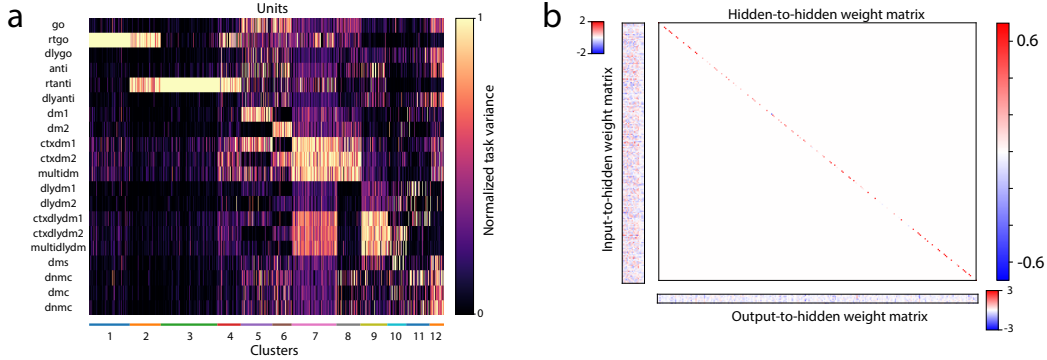


Figure 3: (a) An autapse network from Fig.1 trained on the original 20 Yang tasks showing the formation of 12 specialized clusters; (b) The weights of model including the diagonal hidden to hidden matrix which clearly show the existence of no modular structure.

compared to the fully-connected counterparts. We also compare the performance of these models at the same fixed number of gradient steps early in training to show sample efficiency differences (Fig. 2a, *inset*).

### 2.3 LM-RNNs show that ‘Yang tasks’ are rapidly learned with simple autapse networks

While we demonstrated that LM-RNNs at all  $d$  perform better than fully-connected networks, we particularly note that  $d = 0$ , (i.e., a ‘network’ where each node is only connected to itself; in this case the network is simply a pool of disconnected autapses) also performs better than a fully-connected network in terms of learning speed while reaching the *same asymptotic performance as a larger fully connected network*. Remarkably, as seen in Fig. 3, this pool of autapses continues to show ‘modularity’ in the network through the nodal-task-variance based metrics used in [39] — however this apparent modularity clearly cannot be a result of any modular structures in the network due to the absence of any inter-node network connections.

While these results are in themselves indicative of the advantages conferred by LM-RNNs, we note that the Yang tasks are evidently too simplistic to make any strong claims, since they do not even require a network of neurons to accomplish the task.

### 2.4 Mod-Cog: An expanded battery of cognitive tasks

To perform a more robust demonstration of the utility of LM-RNNs, we construct a battery of new tasks, inspired by cognitive science problems such as interval estimation, mental navigation and sequence generation. We build this series of tasks on the neurogym framework[29] as a set of modular and compositional extensions to the 20 Yang tasks, such that the same input and output space can be utilized across all tasks. In particular, we build extensions, that incorporate additional complexity in two main forms: interval estimation, and sequence generation.

In the case of interval estimation, we consider the set of ‘delay’ based tasks in the Yang tasks. In the Yang tasks, 12 out of 20 tasks involve a delay period in the presented input, wherein the network is expected to persistently hold the input presented in an internal memory before performing a task-relevant computation. To incorporate interval estimation in these tasks, we require the output to be displaced with respect to the originally expected output by a magnitude dependent on the length of the delay period. To this end, we choose the delay length randomly from a uniform distribution (as opposed to the fixed delay length considered in Yang tasks). As representative examples, in Fig. 4a,b we show the inputs and expected outputs for two different delay period lengths in the DlyGo\_IntL task, constructed as an interval estimation extension to the DlyGo task from Yang tasks. For each of the 12 tasks, the interval-dependent-displacement may be either of clockwise or anti-clockwise, resulting in the introduction of 24 new tasks.

In the case of sequence generation, the output of each task is modified to not be a single static direction, but instead a time-varying output corresponding to a drifting direction starting at a particular point

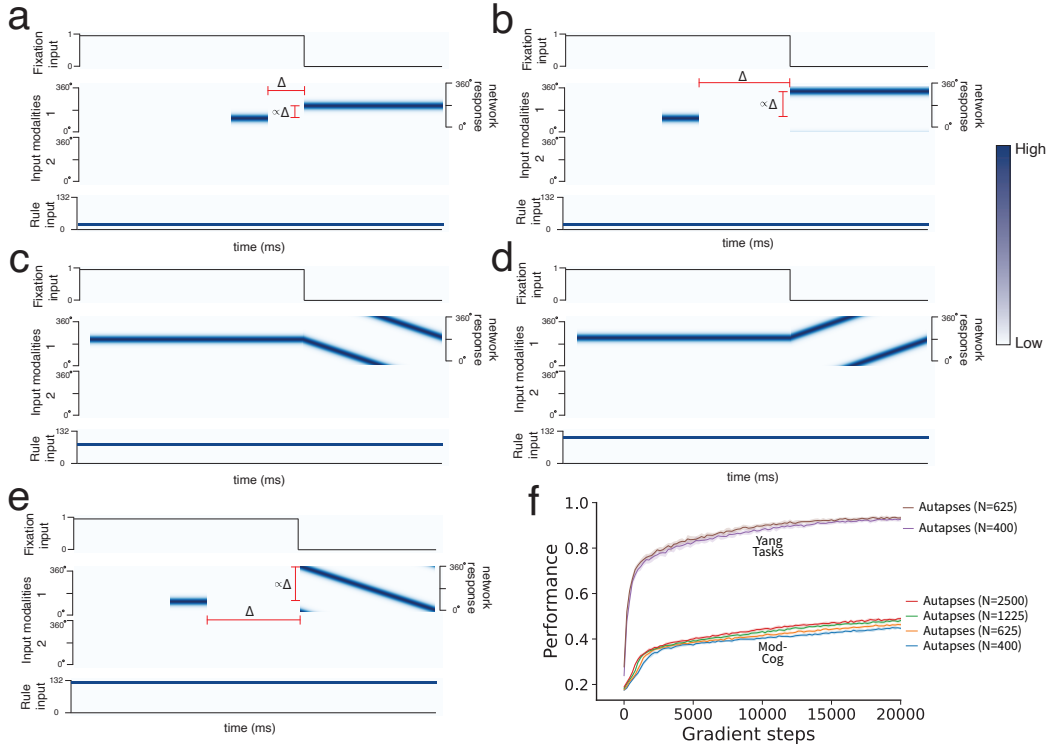


Figure 4: Schematic of the tasks in Mod-Cog, that extend the Yang tasks. (a,b) Tasks DlyGo\_IntL and DlyGo\_IntL as interval estimation extensions to the DlyGo task from Yang tasks for two different lengths of delay periods. (c,d) Tasks Go\_SeqR and Go\_SeqL as sequence generation extensions to the Go task from Yang tasks. (e) The compositional extension DlyGo\_IntL\_SeqR that combines both interval estimation as well as sequence generation. (f) Mod-Cog introduces significantly more complex tasks as compared to Yang tasks, which can no longer be solved by a pool of autapses, irrespective of the size of the pool.

(dependent on the particular task). The direction of drift can be changed dependent on the particular task. As representative examples, in Fig. 4c,d we show the inputs and expected outputs for the Go\_SeqL and Go\_SeqR tasks, constructed as an sequence generation extensions to the Go task from Yang tasks. This introduces 40 new tasks based on the earlier set of 20 tasks, with the output of each task drifting either clockwise or anti-clockwise.

This completes the construction of the 64 new tasks that we use in conjunction with the original 20 tasks as the tasks used for our main set of results hereafter in this paper. We refer to this set of 84 tasks as Mod-Cog. We note however that our modifications to the tasks are modular in nature (which is similar in spirit to the already existing modular subtask structure in the Yang tasks). This allows for an additional extension of 48 more tasks that may be generated by a composition of the sequence generation and interval estimation extensions (such as the DlyGo\_IntL\_SeqR task shown in Fig. 4e). For simplicity, we do not use these additional 48 tasks in our main results; however they are included in the repository of tasks that we provide at github link (will be inserted upon acceptance; provided as .zip file in supplementary material).

The rule input used for Mod-Cog is encoded as a one-hot vector, similar to the setup used in [39]. This ensures that the rule input is not used as a signal to help decompose tasks into having common subtasks.

To demonstrate that Mod-Cog is significantly harder than Yang tasks, we demonstrate in Fig. 4f that a pool of autapses is incapable of achieving significant performance levels, in sharp contrast with the Yang tasks. Moreover, this is independent of the number of autapses — even pools that are  $\sim 6$  times larger than those necessary for solving Yang tasks are unable to produce larger than 50% performance accuracy.

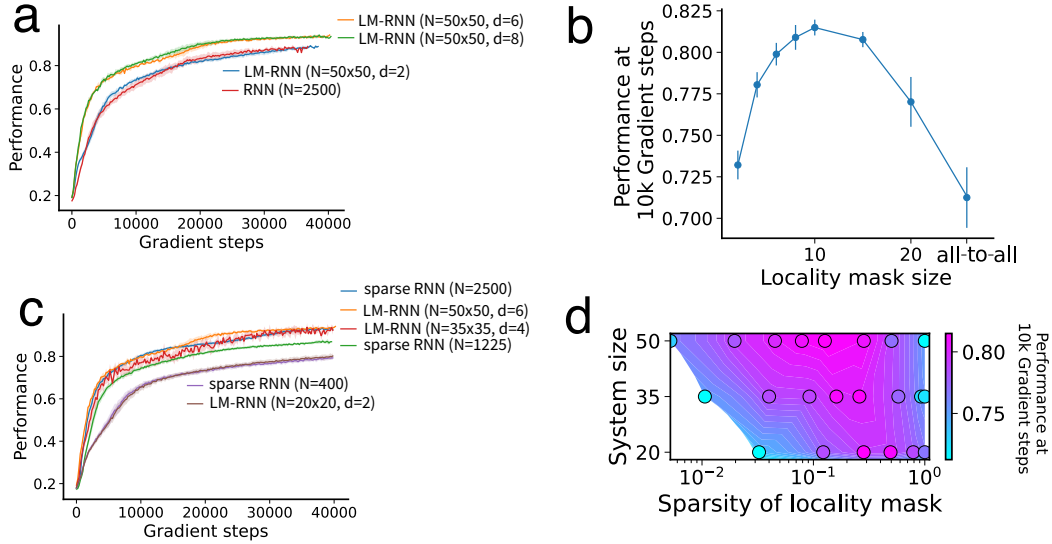


Figure 5: (a) LM-RNNs for all values of  $d$  perform equally well or better than a fully-connected network with the same number of nodes. This improvement takes the form of faster learning as well as better asymptotic performance. (b) Network performance at  $10^4$  gradient steps for different values of  $d$ , demonstrating an optimal locality size that leads to the fastest learning. (c) LM-RNN performance for varying system size for a fixed network sparsity of  $\sim 4\%$ , as compared with fixed random sparse networks with the same sparsity. Performance for sparse RNNs is similar to or only slightly worse than LM-RNNs with the same sparsity (d) Network performance as a function of system size ( $N^2 = \text{System Size}$ ) and sparsity of the locality mask (i.e., the fraction of nonzero entries in the hidden-to-hidden weight matrix). At larger system sizes, the optimal sparsity for best performance is lower.

## 2.5 RNN and LM-RNN performance on Mod-Cog

As earlier, we examine the performance of LM-RNNs with varying  $d$  on Mod-Cog, and compare them with fully-connected RNNs as a function of the number of gradient steps in training (cf. Fig. 5a). Here again we see that LM-RNNs, for appropriately chosen values of  $d$  train significantly more rapidly as compared to fully connected networks. Due to the increased task complexity (as evidenced by Fig. 4f), locality masks corresponding to very small values of  $d$  result in suboptimal performance (which is nonetheless similar to the  $d \rightarrow \infty$  corresponding to the fully connected network). Instead, intermediate small values  $d$  outperform all other values of  $d$ , as shown in Fig. 5b, indicating an optimal nontrivial locality mask  $d$ . For smaller networks, the optimal value of  $d$  corresponds to increasingly larger fractions of all edges in the network (cf. Fig. 5d), indicating that the optimal may depend more directly on the complexity of the tasks to be solved, rather than scaling with the number of nodes in the network.

Remarkably, we note that for most LM-RNNs, a *random* sparse graph with the same number of incoming edges from each node performs almost as well as the graph chosen through locality masking, as shown in Fig. 5c. In each case the locality mask performs slightly better or as well as the random sparse graph, while remaining significantly better than dense fully-connected networks. For the case of small values of  $d$ , we hypothesize that the slight improvement of locality masks may arise from the presence of disconnected components in random sparse graphs in networks with low degrees.

## 2.6 Controls – comparisons with various baselines for sparsity

We perform comparisons across 3 baselines. First, fully-connected networks with the same number of nodes; second, fully-connected networks with the same number of synapses; and third, fully-connected networks with the same number of nodes, but with an additional  $L_1$  regularization term in the loss function to promote the discovery of sparse solutions through training. As we demonstrate in Table 1, LM-RNNs reach a higher performance earlier than all other comparable models. While

	Performance at 10k gradient steps	No. of nonzero weights	No. of nonzero hidden-to-hidden weights
<b>LM-RNN(<math>N = 50 \times 50, d = 6</math>)</b>	<b><math>0.799 \pm 0.007</math></b>	<b><math>6.17 \times 10^5</math></b>	<b><math>2.82 \times 10^5</math></b>
<b>LM-RNN(<math>N = 50 \times 50, d = 10</math>)</b>	<b><math>0.815 \pm 0.005</math></b>	<b><math>1.13 \times 10^6</math></b>	<b><math>7.92 \times 10^5</math></b>
RNN( $N = 676$ )	$0.69 \pm 0.01$	$5.47 \times 10^5$	$4.57 \times 10^5$
RNN( $N = 2500$ )	$0.71 \pm 0.02$	$6.58 \times 10^6$	$6.25 \times 10^6$
$L_1$ RNN( $N = 2500$ ), $\lambda = 10^{-4}$	$0.59 \pm 0.02$	$4.00 \times 10^5$	$6.51 \times 10^4$
$L_1$ RNN( $N = 2500$ ), $\lambda = 10^{-5}$	$0.72 \pm 0.01$	$5.16 \times 10^5$	$1.81 \times 10^5$
$L_1$ RNN( $N = 2500$ ), $\lambda = 10^{-6}$	$0.73 \pm 0.02$	$1.02 \times 10^6$	$6.87 \times 10^5$
$L_1$ RNN( $N = 2500$ ), $\lambda = 10^{-7}$	$0.71 \pm 0.01$	$1.86 \times 10^6$	$1.52 \times 10^6$

Table 1: Comparison of LM-RNN performance as compared with other networks with similar number of trainable parameters and nonzero weights.  $L_1$  RNNs are fully-connected RNNs with an  $L_1$  regularization to promote sparse solutions. In this case, the number of nonzero weights is counted as the number of weights above a certain threshold in the trained RNN.

sparse networks achieved through  $L_1$  regularized models perform better than fully-connected models at some choices of regularization strengths, they achieve this better performance slower than LM-RNNs with static sparsity. Thus while sparsity is clearly beneficial to improved performance in the multitask setting of Mod-Cog, choosing this sparsity in a fixed, task-independent fashion at the start of training results in faster training.

### 3 Discussion

Through our results, we have demonstrated that a simple fixed sparse graph can provide a large increase in the sample-efficiency of the training process in single-layer recurrent networks. These results could in principle be extended to other architectures and tasks but we restricted our experiments to simple RNNs and cognitive tasks for their relevance to systems and computational neuroscience.

We have found that given a certain amount of task complexity and network size, there is an optimal amount of locality masking that provides the most benefit to learning, both in terms of sample efficiency and asymptotic performance. While we have shown this result for recurrent networks, similar results on an optimal value of sparsity have been derived analytically for cerebellum-like feedforward architectures [1, 21]. It remains an open question to theoretically investigate the relationship between task complexity and the amount of sparsity that is needed: if the network is too sparse, it will not have enough expressivity to perform well on the dataset, while if the network is too dense, the benefits provided by sparsity will not be exploited.

Although our matrices are extremely sparse and would be well suited to sparse matrix representations, we still maintain dense matrix datatypes for all of the training and evaluation processes since standard libraries like PyTorch do not have native support for these data structures. As sparse matrices get more common and their usefulness more apparent, as has been pointed out before [22], it will be very useful for native deep learning software and hardware implementations on GPUs to exploit the potential efficiencies of very sparse matrix structures.

### 4 Acknowledgements

We thank Guangyu Robert Yang for open-sourcing the 20 cognitive tasks set and the NeuroGym framework [29] released under the MIT License. This work was supported by the MathWorks Science Fellowship to MK, the Simons Foundation through the Simons Collaboration on the Global Brain, the ONR, and the Howard Hughes Medical Institute through the Faculty Scholars Program to IRF.

## References

- [1] Baktash Babadi and Haim Sompolinsky. Sparseness and expansion in sensory representations. *Neuron*, 83(5):1213–1226, 2014.
- [2] Pedro F. da Costa, Sebastian Popescu, Robert Leech, and Romy Lorenz. Elucidating cognitive processes using lstms. In *Conference on Cognitive Computational Neuroscience*, 2019. URL <https://ccneuro.org/2019/proceedings/0000272.pdf>.
- [3] Pau de Jorge, Amartya Sanyal, Harkirat S Behl, Philip HS Torr, Gregory Rogez, and Puneet K Dokania. Progressive skeletonization: Trimming more fat from a network at initialization. *arXiv preprint arXiv:2006.09081*, 2020.
- [4] Lea Duncker, Laura Driscoll, Krishna V Shenoy, Maneesh Sahani, and David Sussillo. Organizing recurrent network dynamics by task-computation to enable continual learning. In H. Larochelle, M. Ranzato, R. Hadsell, M.F. Balcan, and H. Lin, editors, *Advances in Neural Information Processing Systems*, volume 33, pages 14387–14397. Curran Associates, Inc., 2020. URL <https://proceedings.neurips.cc/paper/2020/file/a576eafbc762079f7d1f77fca1c5cc2-Paper.pdf>.
- [5] Utku Evci, Trevor Gale, Jacob Menick, Pablo Samuel Castro, and Erich Elsen. Rigging the lottery: Making all tickets winners. In *International Conference on Machine Learning*, pages 2943–2952. PMLR, 2020.
- [6] Jonathan Frankle and Michael Carbin. The lottery ticket hypothesis: Finding sparse, trainable neural networks. *arXiv preprint arXiv:1803.03635*, 2018.
- [7] Jonathan Frankle, Gintare Karolina Dziugaite, Daniel M Roy, and Michael Carbin. Stabilizing the lottery ticket hypothesis. *arXiv preprint arXiv:1903.01611*, 2019.
- [8] Song Han, Jeff Pool, John Tran, and William Dally. Learning both weights and connections for efficient neural network. *Advances in neural information processing systems*, 28, 2015.
- [9] Geoffrey Hinton, Oriol Vinyals, Jeff Dean, et al. Distilling the knowledge in a neural network. *arXiv preprint arXiv:1503.02531*, 2(7), 2015.
- [10] John J Hopfield. Neural networks and physical systems with emergent collective computational abilities. *Proceedings of the national academy of sciences*, 79(8):2554–2558, 1982.
- [11] Max Jaderberg, Andrea Vedaldi, and Andrew Zisserman. Speeding up convolutional neural networks with low rank expansions. *arXiv preprint arXiv:1405.3866*, 2014.
- [12] Herbert Jaeger. The “echo state” approach to analysing and training recurrent neural networks—with an erratum note. *Bonn, Germany: German National Research Center for Information Technology GMD Technical Report*, 148(34):13, 2001.
- [13] Steven A Janowsky. Pruning versus clipping in neural networks. *Physical Review A*, 39(12): 6600, 1989.
- [14] Ta-Chu Kao, Kristopher Jensen, Gido van de Ven, Alberto Bernacchia, and Guillaume Hennequin. Natural continual learning: success is a journey, not (just) a destination. *Advances in Neural Information Processing Systems*, 34, 2021.
- [15] Mikail Khona, Sarthak Chandra, and Ila R Fiete. From smooth cortical gradients to discrete modules: spontaneous and topologically robust emergence of modularity in grid cells. *bioRxiv*, pages 2021–10, 2022.
- [16] Diederik P Kingma and Jimmy Ba. Adam: A method for stochastic optimization. *arXiv preprint arXiv:1412.6980*, 2014.
- [17] Aditya Kusupati, Vivek Ramanujan, Raghav Somani, Mitchell Wortsman, Prateek Jain, Sham Kakade, and Ali Farhadi. Soft threshold weight reparameterization for learnable sparsity. In *International Conference on Machine Learning*, pages 5544–5555. PMLR, 2020.

- [18] Yann LeCun, John Denker, and Sara Solla. Optimal brain damage. *Advances in neural information processing systems*, 2, 1989.
- [19] Namhoon Lee, Thalaiyasingam Ajanthan, and Philip Torr. SNIP: SINGLE-SHOT NETWORK PRUNING BASED ON CONNECTION SENSITIVITY. In *International Conference on Learning Representations*, 2019. URL <https://openreview.net/forum?id=B1VZqjAcYX>.
- [20] Namhoon Lee, Thalaiyasingam Ajanthan, Stephen Gould, and Philip H. S. Torr. A signal propagation perspective for pruning neural networks at initialization. In *International Conference on Learning Representations*, 2020. URL <https://openreview.net/forum?id=HJeTo2VFwH>.
- [21] Ashok Litwin-Kumar, Kameron Decker Harris, Richard Axel, Haim Sompolinsky, and LF Abbott. Optimal degrees of synaptic connectivity. *Neuron*, 93(5):1153–1164, 2017.
- [22] Shiwei Liu, Decebal Constantin Mocanu, Yulong Pei, and Mykola Pechenizkiy. Selfish sparse rnn training. In *International Conference on Machine Learning*, pages 6893–6904. PMLR, 2021.
- [23] Christos Louizos, Max Welling, and Diederik P Kingma. Learning sparse neural networks through  $l_0$  regularization. *arXiv preprint arXiv:1712.01312*, 2017.
- [24] Mantas Lukoševičius and Herbert Jaeger. Reservoir computing approaches to recurrent neural network training. *Computer Science Review*, 3(3):127–149, 2009.
- [25] Wolfgang Maass. Liquid state machines: motivation, theory, and applications. *Computability in context: computation and logic in the real world*, pages 275–296, 2011.
- [26] Wolfgang Maass, Thomas Natschläger, and Henry Markram. Real-time computing without stable states: A new framework for neural computation based on perturbations. *Neural computation*, 14(11):2531–2560, 2002.
- [27] Nicolas Y Masse, Matthew C Rosen, Doris Y Tsao, and David J Freedman. Rapid learning with highly localized synaptic plasticity. *bioRxiv*, 2022.
- [28] Decebal Constantin Mocanu, Elena Mocanu, Phuong H Nguyen, Madeleine Gibescu, and Antonio Liotta. A topological insight into restricted boltzmann machines. *Machine Learning*, 104(2):243–270, 2016.
- [29] Manuel Molano-Mazon, Joao Barbosa, Jordi Pastor-Ciurana, Marta Fradera, Ru-Yuan Zhang, Jeremy Forest, Jorge del Pozo Lerida, Li Ji-An, Christopher J Cueva, Jaime de la Rocha, et al. Neurogym: An open resource for developing and sharing neuroscience tasks. 2022.
- [30] Eli Moore and Rishidev Chaudhuri. Using noise to probe recurrent neural network structure and prune synapses. In H. Larochelle, M. Ranzato, R. Hadsell, M.F. Balcan, and H. Lin, editors, *Advances in Neural Information Processing Systems*, volume 33, pages 14046–14057. Curran Associates, Inc., 2020. URL <https://proceedings.neurips.cc/paper/2020/file/a1ada9947e0d683b4625f94c74104d73-Paper.pdf>.
- [31] Michael C Mozer and Paul Smolensky. Using relevance to reduce network size automatically. *Connection Science*, 1(1):3–16, 1989.
- [32] Sharan Narang, Erich Elsen, Gregory Diamos, and Shubho Sengupta. Exploring sparsity in recurrent neural networks. *arXiv preprint arXiv:1704.05119*, 2017.
- [33] Reidar Riveland and Alexandre Pouget. A neural model of task compositionality with natural language instructions. *bioRxiv*, 2022.
- [34] Peter J Rousseeuw. Silhouettes: a graphical aid to the interpretation and validation of cluster analysis. *Journal of computational and applied mathematics*, 20:53–65, 1987.
- [35] Pedro Savarese, Hugo Silva, and Michael Maire. Winning the lottery with continuous sparsification. *Advances in Neural Information Processing Systems*, 33:11380–11390, 2020.

- [36] Hidenori Tanaka, Daniel Kunin, Daniel L Yamins, and Surya Ganguli. Pruning neural networks without any data by iteratively conserving synaptic flow. In H. Larochelle, M. Ranzato, R. Hadsell, M.F. Balcan, and H. Lin, editors, *Advances in Neural Information Processing Systems*, volume 33, pages 6377–6389. Curran Associates, Inc., 2020. URL <https://proceedings.neurips.cc/paper/2020/file/46a4378f835dc8040c8057beb6a2da52-Paper.pdf>.
- [37] Chaoqi Wang, Guodong Zhang, and Roger Grosse. Picking winning tickets before training by preserving gradient flow. In *International Conference on Learning Representations*, 2020. URL <https://openreview.net/forum?id=SkgsACVKPH>.
- [38] Wei Wen, Yuxiong He, Samyam Rajbhandari, Minjia Zhang, Wenhan Wang, Fang Liu, Bin Hu, Yiran Chen, and Hai Li. Learning intrinsic sparse structures within long short-term memory. In *International Conference on Learning Representations*, 2018. URL <https://openreview.net/forum?id=rk6cfpRjZ>.
- [39] Guangyu Robert Yang, Madhura R Joglekar, H Francis Song, William T Newsome, and Xiao-Jing Wang. Task representations in neural networks trained to perform many cognitive tasks. *Nature neuroscience*, 22(2):297–306, 2019.
- [40] Hattie Zhou, Janice Lan, Rosanne Liu, and Jason Yosinski. Deconstructing lottery tickets: Zeros, signs, and the supermask. *Advances in neural information processing systems*, 32, 2019.
- [41] Julian Georg Zilly, Rupesh Kumar Srivastava, Jan Koutník, and Jürgen Schmidhuber. Recurrent highway networks. In *International conference on machine learning*, pages 4189–4198. PMLR, 2017.

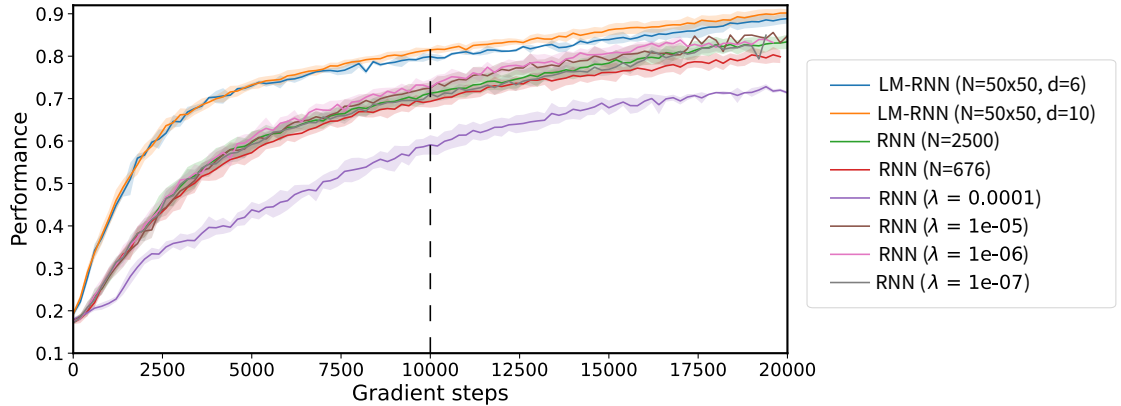


Figure 6: **Performance curves** of models trained with varying values of sparsity (L1) regularization showing that a fixed local mask (of similar sparsity, cf. Table 1) is better.

## A Methods and Hyperparameters

PyTorch was used for all simulations. All networks were trained with supervised learning using a cross entropy loss. The optimizer used was Adam [16] with a learning rate of  $10^{-3}$ . Each trial was drawn randomly and independently and the tasks were randomly interleaved. The Neurogym [29] environment was used to create tasks and the training data for the model.

For every performance curve, we trained 15 RNNs with different random seeds and used the averaged curve for plotting and computing the optimal locality mask sizes.

An expanded description of the Mod-Cog tasks and how to create them will be made available at the Github repository after acceptance.

## B Formation of clusters in LM-RNNs

To measure the number of clusters that the hidden nodes of the RNN partition into to solve a task, we first use agglomerative hierarchical clustering<sup>1</sup> to obtain a linkage tree for the variance of each node across different inputs for a given task. Then, the silhouette score [34] is evaluated for each possible linkage-based cluster partition and the partition with the highest score is selected to represent the clustering of the RNN.

Through figures 7,8,9,10, 11, 12 we show that LM-RNNs at the optimal locality mask size  $d$  form a more optimal number of clusters that correspond better to the modular subtask structure present. For example, for LM-RNN( $N = 50^2$ ,  $d = 10$ ) Fig.11, a single module (module #15) is involved solely with right-ward sequence generation. In contrast, for the fully connected RNN( $N = 2500$ ) Fig.12, multiple modules (module #18, #23, #24, #25) are required for the same subtask.

<sup>1</sup><https://docs.scipy.org/doc/scipy/reference/generated/scipy.cluster.hierarchy.linkage.html>

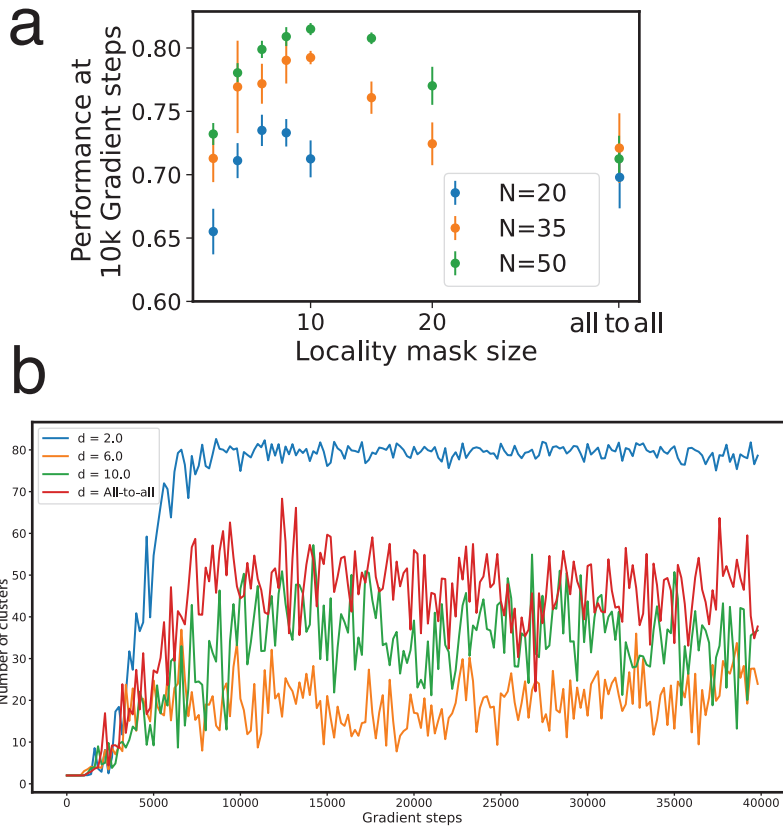


Figure 7: (a) Performance at 10k gradient steps for networks of sizes (400,1225,2500) on 84 tasks showing optimal locality mask sizes; (b) for LM-RNNs with  $20 \times 20$  nodes, the number of clusters obtained by agglomerative hierarchical clustering over training shows that the more optimal locality masked networks discover a lower, more appropriate number of clusters which seems to qualitatively correspond to the modular subtask structures in Mod-Cog.

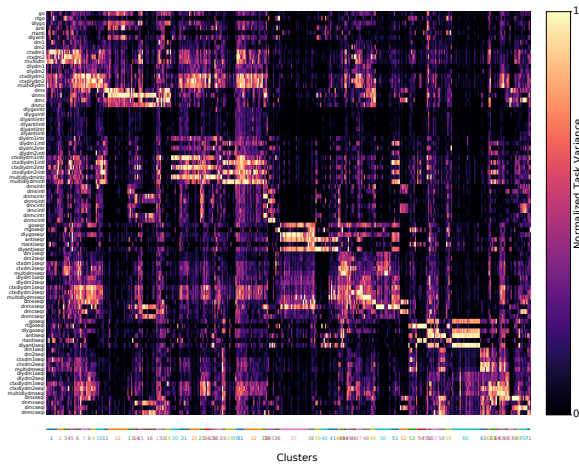


Figure 8: An LM-RNN( $N=20 \times 20, d=2$ ) trained on 84 Mod-Cog tasks showing the formation of clusters

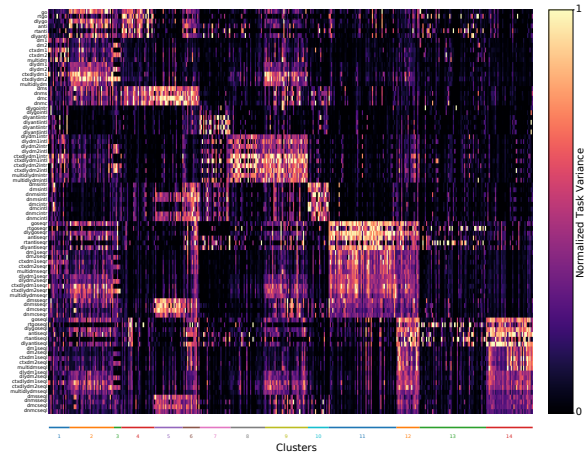


Figure 9: An LM-RNN(N=20x20,d=6) trained on 84 Mod-Cog tasks showing the formation of clusters

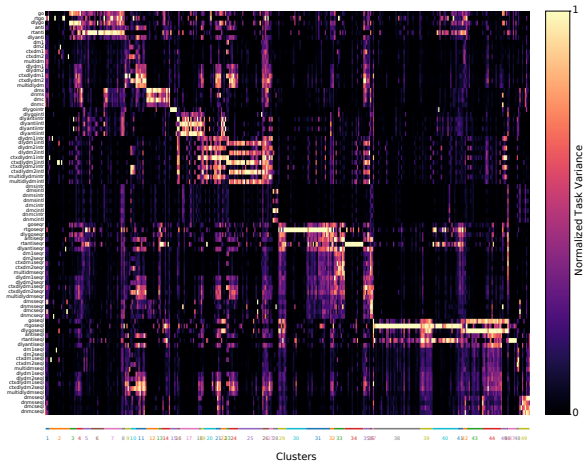


Figure 10: An RNN(N=400) trained on 84 Mod-Cog tasks showing the formation of clusters

